

Self-Cleaning Membrane to Extend the Lifetime of an Implanted Glucose Biosensor

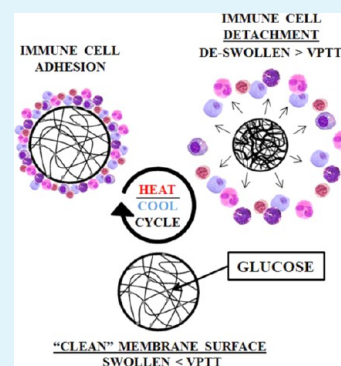
Alexander A. Abraham,[†] Ruochong Fei,[†] Gerard L. Coté,[†] and Melissa A. Grunlan^{*,†,‡}

[†]Department of Biomedical Engineering, Texas A&M University, College Station, Texas 77843-3120, United States

[‡]Materials Science and Engineering Program, Texas A&M University, College Station, Texas 77843-3120, United States

Supporting Information

ABSTRACT: The lifetime and efficacy of a subcutaneously implanted glucose biosensor could be greatly improved by a self-cleaning membrane capable of periodic physical removal of adhered cells associated with the foreign body reaction. Previously, we reported a thermoresponsive double network nanocomposite (DNNC) membrane composed of poly(*N*-isopropylacrylamide) (PNIPAAm) and embedded polysiloxane nanoparticles. When the membrane was thermally cycled above and below its volume phase transition temperature (VPTT, $\sim 33\text{--}35\text{ }^{\circ}\text{C}$), the associated deswelling and reswelling, respectively, led to in vitro cell release. Herein, this membrane design was tailored to meet the specific demands of a subcutaneously implanted glucose biosensor, and critical functional properties were assessed. First, *N*-vinylpyrrolidone (NVP) comonomer increased the VPTT to $\sim 38\text{ }^{\circ}\text{C}$ so that the membrane would be swollen and thus more permeable to glucose in the “off-state” (i.e., no heating) while residing in the subcutaneous tissue ($\sim 35\text{ }^{\circ}\text{C}$). Second, glucose diffusion kinetics through the DNNC membrane was experimentally measured in its deswollen and reswollen states. A cylindrical DNNC membrane with dimensions considered suitable for implantation ($1.5 \times 5\text{ mm}$, diameter \times length) was used to model the glucose diffusion lag time. In addition, the DNNC cylinder was used to observe dimensional changes associated with deswelling and reswelling. Noncytotoxicity was confirmed and self-cleaning was assessed in vitro in terms of thermally driven cell release to confirm the potential of the DNNC membrane to control biofouling.



KEYWORDS: thermoresponsive, hydrogel, nanocomposite, glucose diffusion, biofouling, cell release

INTRODUCTION

In the United States alone, diabetes mellitus affects ~ 26 million individuals and is projected to increase to ~ 36 million by 2030.¹ Poor monitoring of glucose levels leads to an increase in hypo- or hyperglycemic events as well as serious long-term complications (e.g., blindness and heart disease) or even death.² Presently, a finger-prick test is most commonly used to provide intermittent blood sugar measurements. However, a subcutaneously implanted glucose biosensor could offer a continuous and more convenient method to monitor glucose levels. Unfortunately, membrane biofouling severely limits the lifetime and accuracy of subcutaneous or transdermal sensors.^{3,4} Upon implantation of a sensor, a foreign body reaction is triggered that results in the attachment of proteins and cells to the surrounding membrane and, eventually, the formation of a fibrous capsule^{3,4} (Figure 1). Membrane biofouling will inhibit glucose diffusion to the sensor thereby causing its failure. In this way, commercially available transdermal continuous glucose monitoring (CGM) systems are limited to a 3–7 day lifetime. Approaches to control membrane biofouling have largely focused on passive or “anti-fouling” membranes such as those based on poly(ethylene glycol)diacrylate (PEG-DA),⁵ poly(hydroxyethylmethacrylate) (PHEMA),⁶ and poly(tetrafluoroethylene) (PTFE).^{7,8} In contrast, the self-cleaning membrane reported herein relies on an active or “foul-releasing” mechanism to physically remove adsorbed cells.

Thermoresponsive poly(*N*-isopropylacrylamide) (PNIPAAm) hydrogels undergo deswelling and reswelling when heated above and cooled below, respectively, their volume phase transition temperature (VPTT) ($\sim 33\text{--}35\text{ }^{\circ}\text{C}$). This process has been shown to cause the release of cultured cells in vitro.^{9–14} If utilized as a membrane for an implanted glucose biosensor, self-cleaning may be accomplished via transdermal thermal cycling. Conventional single network (SN) PNIPAAm hydrogels prepared via copolymerization of NIPAAm and a cross-linker such as *N,N'*-methylenebisacrylamide (BIS) exhibit slow deswelling and reswelling kinetics (i.e., thermosensitivity) as well as poor mechanical properties.^{15,16} When used as a self-cleaning membrane, the PNIPAAm hydrogel requires enhanced thermosensitivity (for self-cleaning) as well as robust mechanical properties (for surgical insertion). Recently, we reported a double network nanocomposite (DNNC) hydrogel composed of an interpenetrating, asymmetrically cross-linked PNIPAAm matrix with polysiloxane nanoparticles ($\sim 200\text{ nm}$ diameter) embedded during formation of the first network.¹⁷ This DNNC hydrogel exhibited significantly improved thermosensitivity in terms of both the rate and the extent of deswelling and reswelling versus a conventional PNIPAAm

Received: May 27, 2013

Accepted: December 4, 2013

Published: December 4, 2013

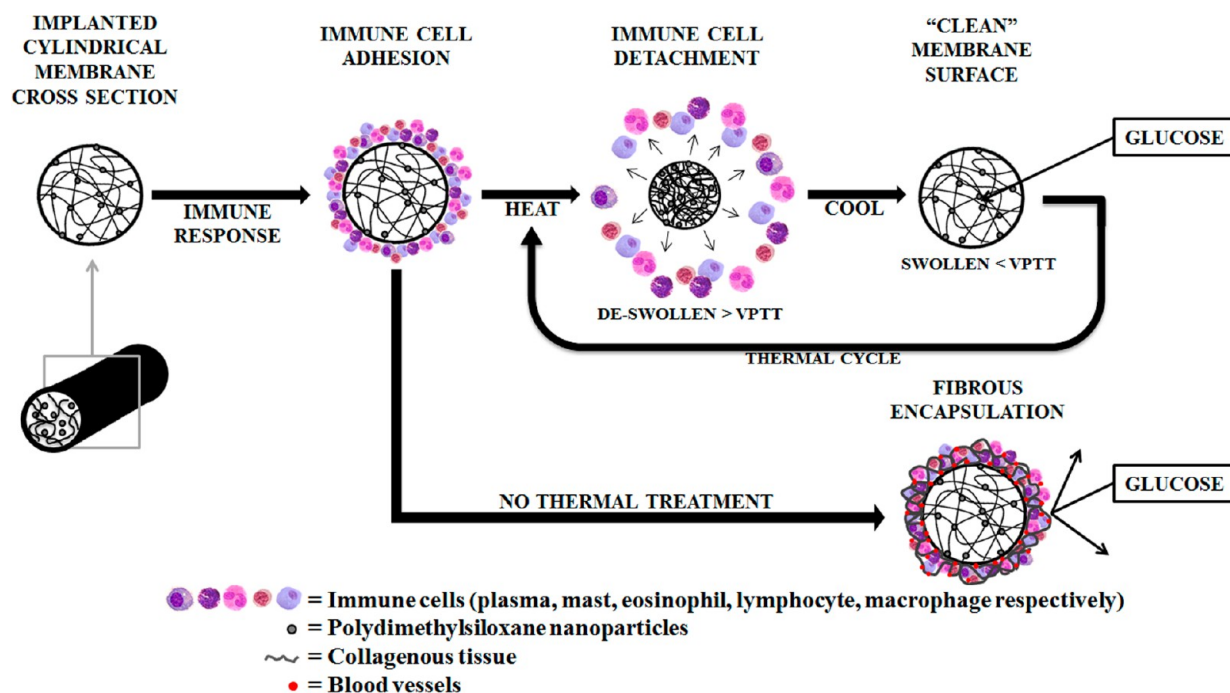


Figure 1. Biofouling of a membrane surrounding an implanted biosensor compromises glucose diffusion. The double network nanocomposite (DNNC) membrane described herein is designed to exhibit “self-cleaning” when thermally cycling above its volume phase transition temperature (VPTT).

hydrogel. Furthermore, the DNNC hydrogel exhibited improved modulus and strength.

Extending the utility of this DNNC hydrogel as a self-cleaning membrane for an implanted glucose biosensor requires further refinement and is addressed in this study. First, the VPTT of the DNNC membrane was increased to ~ 38 °C. In the subcutaneous tissue of the wrist, a likely location for an implanted sensor, the body temperature is ~ 35 °C.^{18,19} Thus, a membrane with a VPTT ~ 38 °C in the “off-state” will be fully swollen for optimal glucose diffusion. When undergoing self-cleaning (“on-state”), the membrane would begin to deswell via transdermal heating. Copolymerization of NIPAAm with a hydrophilic comonomer is known to increase the VPTT of the resulting hydrogel.^{20,21} Previously, we demonstrated that addition of 1–2 wt % *N*-vinylpyrrolidone (NVP) comonomer (based on NIPAAm wt) produced analogous single network nanocomposite (SNNC) hydrogels with a VPTT of ~ 38 °C.²² Thus, NVP was similarly incorporated into the DNNC hydrogels. Second, glucose diffusion through a planar DNNC membrane was measured at temperatures above and below the VPTT. Third, a membrane with a geometry suitable for implantation was considered to be a cylindrical rod (~ 1.5 mm \times 5 mm, diameter \times length) (Figure 2). A finite element model

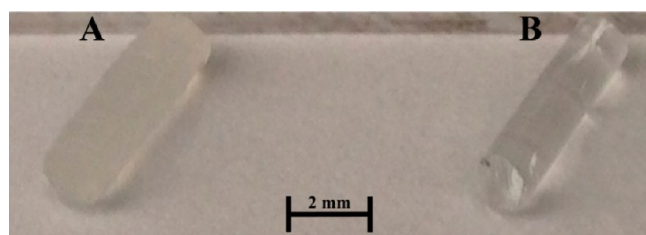


Figure 2. DNNC [A] and PEG-DA [B] cylindrical membranes fabricated with a diameter of ~ 1.5 mm and length of 5 mm.

was constructed for the DNNC hydrogel cylinders to estimate the glucose diffusion lag time before achieving equilibrium with its external environment at varying glucose concentrations. Since size and geometry also affect thermosensitivity^{23,24} which are critical to fast and efficient self-cleaning, the thermosensitivity of the DNNC hydrogel cylinders was assessed by measuring the change in diameter with temperature. Finally, cytocompatibility was assessed and thermally induced in vitro cellular detachment was observed using planar DNNC hydrogels.

MATERIALS AND METHODS

Materials. NIPAAm (97%), NVP, PEG-DA (MW 575 g/mol), ammonium hydroxide (NH₄OH), sodium chloride (NaCl), sodium phosphate-dibasis (Na₂HPO₄), potassium phosphate-monobasis (KH₂PO₄), hydrochloric acid (HCl), sodium hydroxide (NaOH), newborn calf serum (NCS), antibiotic antimycotic solution (100 \times) (stabilized bioreagent sterile filtered with 10 000 units of penicillin and 10 mg of streptomycin A), sterile Dulbecco’s phosphate buffered saline (PBS), HEPES ($\geq 99.5\%$), and Dulbecco’s Modified Eagle’s Medium (DMEM) (1000 mg dL⁻¹ glucose and L-glutamine without sodium bicarbonate and phenol red) were purchased from Sigma-Aldrich (St. Louis, MO). Potassium chloride (KCl) and D-glucose anhydrous was purchased from Fisher Scientific (Pittsburgh, PA). Potassium persulfate (K₂S₂O₈) was purchased from Mallinckrodt Chemicals. *N,N'*-Methylenebisacrylamide (BIS, 99%) was purchased from Acros Organics (Geel, Belgium). 2-Hydroxy-2-methyl-1-phenyl-1-propanone (Darocur 1173) and 1-[4-(2-Hydroxy)-phenyl]-2-hydroxy-2-methyl-1-propane-1-one (Irgacure 2959) was purchased from Ciba Specialty Chemicals (Tarrytown, NY). Octamethylcyclotetrasiloxane (D₄) and 1,3,5,7-tetramethyl-1,3,5,7-tetravinylcyclotetrasiloxane (D₄^{VI}) came from Gelest, Inc. Dodecylbenzenesulfonic acid (DBSA, BIO-SOFT S-101) came from Stepan Co. (Northfield, IL). The Slide-A-Lyzer dialysis cassettes (MWCO 10 000) and lactate dehydrogenase (LDH) cytotoxicity assay kit were obtained from Pierce (Rockford, IL). For hydrogel fabrication and other experiments, deionized water (DI H₂O) with a resistance of 18 M Ω -cm (Millipore, Billerica, MA) was used. 3T3 H2B-GFP mouse fibroblast cell line was a kind gift from Peter

Ghazal at the Division of Pathway Medicine at the University of Edinburgh. Cell culture media was pH adjusted with 1 M HCl and 1 M NaOH, verified with a pH meter (420 A+, Orion; electrode 5990-30, Cole-Parmer, Vernon Hills, IL), and sterilized by 0.2 μm filtration (sterile 90 mm filter unit, Nalgene Filtration Products).

Preparation of Polysiloxane Nanoparticles. Polysiloxane colloidal nanoparticles with an average diameter of ~ 200 nm were prepared via emulsion polymerization and purified via dialysis as previously reported.¹⁴ The final emulsion was 4.8 wt % solids.

Preparation of PEG-DA Hydrogels. Precursor solutions were formed by vortexing DI-H₂O, PEG-DA (100%v/v), and Darocur 1173 (1% v/v) for 1 min.

Planar Sheets. Planar hydrogel sheets (~ 1 mm thick per electronic caliper measurements) were prepared by pipetting the precursor solution between two clamped glass slides (75 \times 50 mm) separated by polycarbonate spacers (1 mm thick) and exposing the mold to longwave ultraviolet (UV) light (UVP UV-Transilluminator, 6 mW cm^{-2} , $\lambda_{\text{peak}} = 365$ nm) for 2 min at room temperature (RT). Hydrogel sheets were removed from their molds, rinsed with DI H₂O, and soaked in a Petri dish containing DI H₂O (60 mL) for 24 h.

Cylinders. Cylindrical hydrogels (~ 1.5 mm \times 5 mm, diameter \times length per electronic caliper) were prepared by pipetting the precursor solution into a hollow cylindrical glass mold (inside diameter = 1.0 mm, length = 15 mm) with one end sealed by Parafilm. After sealing the other end of the mold, it was likewise exposed to longwave UV light as above at RT for 3 s. The cylindrical hydrogel was removed from the mold, rinsed with DI H₂O, and immersed in a Petri dish containing DI H₂O (60 mL) for 24 h. A clean razor blade was used to equally trim the ends to reduce the length to 5 mm.

Preparation of Thermoresponsive DNNC Hydrogels. DNNC hydrogels were prepared by sequential formation of a relatively tightly cross-linked first network containing polysiloxane nanoparticles (2 wt % solid nanoparticles based on NIPAAm weight) and a loosely cross-linked second network.¹⁷ The "1st network precursor solution" was formed by combining NIPAAm monomer (1.0 g), NVP comonomer (0.16 g), BIS cross-linker (0.04 g), polysiloxane nanoparticle emulsion (0.485 g), Irgacure-2959 photoinitiator (0.08 g), and DI H₂O (6.54 g). The "2nd network precursor solution" was formed by combining NIPAAm (6.0 g), NVP (0.96 g), BIS (0.012 g), Irgacure 2959 (0.24 g), and DI H₂O (21.0 g).

Planar Sheets. Planar hydrogel sheets (1 mm thick) were produced by pipetting the first network precursor solution into a mold consisting of two clamped glass slides (75 \times 50 mm) separated by 1 mm thick polycarbonate spacers. The mold was then immersed into an ice water bath (~ 7 °C) and exposed to longwave UV light for 30 min. The resulting single network nanocomposite (SNNC) sheet was removed from the mold, rinsed with DI H₂O, and then soaked in DI H₂O at RT for 2 days with daily water changes. The SNNC sheet was then transferred into a covered Petri dish containing the second network precursor solution for 24 h at RT. Next, the planar hydrogel was placed into a rectangular mold (1.5 mm thick), photocured for 30 min, and finally soaked in DI H₂O as above.

Cylinders. Cylindrical hydrogels (~ 1.5 mm \times 5 mm, diameter \times length) were prepared by pipetting the precursor solution into a cylindrical glass mold (inside diameter = 1.0 mm, length = 15 mm) as above. The mold was immersed in an ice water bath (~ 7 °C) and exposed for 10 min to longwave UV light. Cylindrical hydrogels were removed from their molds, rinsed with DI H₂O, and soaked in a Petri dish containing DI H₂O (60 mL) for 2 days at RT with daily water changes. A SNNC cylindrical hydrogel was then transferred into a Petri dish containing the second network precursor solution for 24 h at RT. The cylindrical hydrogel was then placed into a second cylindrical mold (diameter = 1.5 mm, length = 15 mm), submerged in an ice water bath (~ 7 °C), exposed for 10 min to longwave UV light, and soaked in DI H₂O as above. A clean razor blade was used to trim ends to reduce the cylindrical length to 5 mm. The final diameter was measured via calipers.

Differential Scanning Calorimetry (DSC). The VPTT of swollen hydrogels was determined by differential scanning calorimetry (DSC, TA Instruments Q100). Water-swollen hydrogels were blotted with a

Kim Wipe, and a small piece was sealed in a hermetic pan. After cooling to -50 °C, the temperature was increased to 50 °C at a rate of 3 °C/min for 2 cycles. The resulting endothermic phase transition peak is characterized by the initial temperature, at which the endotherm starts (T_o), and the peak temperature of the endotherm (T_{max}). Reported data are from the second cycle.

Glucose Diffusion. Planar hydrogel strips (1 cm \times 1 cm \times 1 mm) were placed in a side-by-side diffusion cell (PermeGear, Bethlehem, PA) positioned atop a stir plate. The donor chamber contained 3 mL of glucose solution (~ 1000 mg dL^{-1}), and the receptor chamber contained 3 mL of DI H₂O. Chamber solutions were stirred with Teflon-coated stir bars (800 rpm) to maintain constant solution concentrations. A water jacket maintained the designated temperature (25, 35, and 40 °C) throughout the system. Every 20 min (for a total time of 3 h), 50 μL aliquots were removed via pipet from each chamber and glucose concentration was determined with a YSI 2700 Select Biochemistry Analyzer (YSI Incorporated, Yellow Springs, OH). The diffusion coefficients were calculated using Fick's second law of diffusion.

Glucose Diffusion Lag Time. A computational model of the DNNC hydrogels was developed using COMSOL Multiphysics software (COMSOL, Inc., Los Angeles, CA). Conducting a time-dependent transport of diluted species study, a geometric cylinder (1.5 mm \times 5 mm, diameter \times length) was constructed with a maximum and minimum free tetrahedral mesh element size of 0.382 and 0.0249 mm, respectively. The simulation began with a DNNC hydrogel internal glucose quantity of 0 mg dL^{-1} and external glucose levels of 60, 80, 160, and 300 mg dL^{-1} . The average glucose concentration within the cylindrical hydrogel was assessed every second for 1 h for each external glucose concentration. The diffusion lag time was defined as the time required for the hydrogel internal glucose concentration to fall within 5% of the external glucose concentration.

Thermosensitivity. Three cylindrical DNNC hydrogels (~ 1.5 mm \times 3 mm, diameter \times length) were vertically attached to a single Petri dish with a small amount of optical adhesive (Norland Optical Adhesive 61) to the base of one end. To hydrate the affixed cylinders, the Petri dish was filled with DI H₂O for at least 12 h at RT prior to thermally cycling. The Petri dish was positioned atop a heating plate under a noninverted bright field microscope (Nikon Eclipse LV 100D, Nikon America Inc., Melville, NY) with a 5 \times objective. Images were taken every 5 min as the hydrogels were thermally cycled between 25 and 40 °C for 5 cycles. The average rate of heating to 40 °C was ~ 1.06 °C/min, and passive cooling to 25 °C was ~ 0.28 °C/min. Thus, each cycle consisted of a 1 h heating period followed by 1 h of passive cooling. Cylinder diameters were recorded with Nikon NIS Elements imaging software.

Cytocompatibility. DNNC hydrogel cytocompatibility was assessed by measuring LDH concentrations released by 3T3 H2B-GFP mouse fibroblast cells 24 h after cell seeding versus that of two cytocompatible controls, a PEG-DA hydrogel as well as tissue culture plastic (i.e., polystyrene, PS). Planar DNNC and PEG-DA hydrogel sheets were prepared as described above. Four 6 mm discs were punched from each sheet and then sterilized by immersion in 80% ethanol for 45 min. The hydrogel discs were sequentially washed 3 \times (30 min each) with sterile DMEM (40% NCS), submerged in DMEM (40% NCS) for 24 h, and transferred to a sterile 12-well plate. Next, 3T3 H2B-GFP mouse fibroblast cells [suspended in DMEM (40% NCS) containing antimycotics and antibiotics] were seeded onto each of the hydrogel surfaces and into the empty tissue culture plastic wells at a concentration of ~ 6500 cells cm^{-2} . Cells were allowed to incubate for 24 h at ~ 37 °C ($T < \text{VPTT}$; swollen state) with 5% CO₂. Finally, the media surrounding the hydrogel discs or from the empty wells was extracted and assessed for LDH levels per the manufacturer's protocol. The relative LDH activity was calculated by normalizing PEG-DA and DNNC sample absorptions to that of polystyrene.

"Self-Cleaning" Behavior in Vitro. Planar DNNC and PEG-DA hydrogel sheets (2 cm \times 2 cm \times ~ 1 mm) were sterilized by immersion in 80% ethanol for 45 min. All specimens were then washed 3 \times for 30 min each with sterile DMEM (40% NCS). DNNC and PEG-DA hydrogel sheets were submerged for 48 and 96 h, respectively, in

DMEM (40% NCS). Next, in a sterile plastic Petri dish, DNNC and PEG-DA hydrogel sheets were inoculated with 3T3 H2B-GFP mouse fibroblast cells stained with a lipophilic indocarbocyanine dye (DiI) and suspended in DMEM (40% NCS) containing antimycotics and antibiotics at a concentration of $\sim 30\,000$ cells/mL. For DNNC and PEG-DA hydrogels, cells were allowed to incubate for 4 and 72 h, respectively, at ~ 35 °C ($T < \text{VPTT}$; swollen state) with 5% CO_2 before imaging. The Petri dish was transferred to the enclosed microscope stage which contained two heating pads (Minco) connected to thermistors controlled via a temperature feedback system (LabView). Hydrogel surface images were captured every 20 s for 10 min with an inverted bright field microscope (Nikon Eclipse TE 2000-S, Nikon America Inc., Melville, NY) with a 10 \times objective as the temperature was increased from ~ 35 °C to ~ 39.5 °C ($T > \text{VPTT}$) at a rate of ~ 0.41 °C/min (i.e., ~ 10 min).

RESULTS AND DISCUSSION

VPTT. By incorporating low levels of NVP comonomer (1.6 wt % based on NIPAAm monomer weight) into the first and second network precursor solutions, the VPTT of the DNNC hydrogel was successfully increased. Per the DSC thermogram (Figure S1, Supporting Information), T_o and T_{max} were equal to 36.5 and 39.5 °C, respectively. Thus, at subcutaneous body temperature of the wrist (~ 35 °C), the DNNC hydrogel are expected to be swollen in the absence of external heating (i.e., “off-state”).

Glucose Diffusion. A side-by-side diffusion cell system was used to study glucose diffusion through the DNNC membrane at 25 °C ($T < \text{VPTT}$), 35 °C (body temperature), and 40 °C ($T > \text{VPTT}$). Fick’s second law of diffusion was used to calculate the diffusion coefficients at each temperature:

$$\frac{\partial c}{\partial t} = D \frac{\partial^2 c}{\partial x^2}$$

where c is the concentration within the hydrogel, t is the time, D is the diffusion coefficient, and x is the diffusion distance.^{25–28} Assuming that each solution preserved a uniform concentration and that each element concentration was equal at the hydrogel membrane surface as in the bulk volume of each chamber, the equation may be simplified to

$$Q_t = \frac{ADC_1}{L} \left(t - \frac{L^2}{6D} \right)$$

where Q_t is the overall quantity of glucose transferred through the hydrogel until the specified time, t , A refers to the hydrogel area exposed to the donor or receptor chambers, C_1 is the initial solute concentration of the donor chamber, and L is the measured hydrogel membrane thickness.

Table 1 reveals the influence of temperature on the diffusion coefficients (D) of the DNNC hydrogel. At 25 °C ($T < \text{VPTT}$), the swollen state of the hydrogel facilitates glucose diffusion. In contrast, when heated to 40 °C ($T > \text{VPTT}$), the hydrogel is deswollen and glucose diffusion is thus substantially slowed. While still below the measured T_o of the VPTT (~ 36.5 °C), glucose diffusion at 35 °C (body temperature) began to

Table 1. Glucose Diffusion Coefficients (D) of the DNNC Hydrogel (VPTT ~ 38 °C) at Varying Temperatures

temperature (°C)	membrane behavior	diffusion coefficient (cm^2/s)
25 ($T < \text{VPTT}$)	swollen	$2.73 \pm 0.01 \times 10^{-6}$
35 (body temperature)	swollen	$1.88 \pm 0.01 \times 10^{-6}$
40 ($T > \text{VPTT}$)	deswollen	$1.03 \pm 0.01 \times 10^{-6}$

decrease somewhat indicating that some deswelling may have occurred. However, D of glucose through the dermis and epidermis has been reported as $2.64 \pm 0.42 \times 10^{-6}$ and $0.075 \pm 0.05 \times 10^{-6}$ cm^2/s , respectively.²⁹ Thus, D of glucose through the hydrogel ($1.88 \pm 0.01 \times 10^{-6}$ cm^2/s) is within the functional range. Furthermore, D of a PEG-DA (MW 575 g/mol) hydrogel was previously determined to be $1.59 \pm 0.42 \times 10^{-6}$ cm^2/s ,³⁰ and such materials are noted to not significantly impede glucose transfer to encapsulated biosensors.³¹ Thus, in the “off-state”, glucose diffusion through the DNNC hydrogel to the enclosed sensor is expected to be satisfactory.

A COMSOL Multiphysics computational model was utilized to evaluate the glucose diffusion lag time for a DNNC cylindrical hydrogel. The simulation began with an initial glucose quantity of 0 mg dL^{-1} within the hydrogel and the hydrogel then suspended in an environment with a constant glucose level of varying concentrations: 60, 80, 160, and 300 mg dL^{-1} . These concentrations represent low, normal, high, and very high physiologically glucose levels, respectively.³² Figure 3

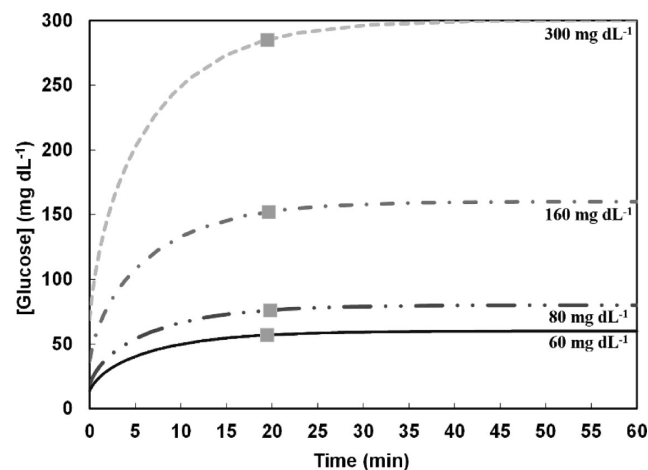


Figure 3. A computational model was utilized to determine the average glucose concentration inside a DNNC cylindrical hydrogel at 35 °C for constant environmental glucose levels of 300, 160, 80, and 60 mg dL^{-1} . The glucose diffusion lag time (gray ■) marks when the average internal hydrogel glucose concentration is 95% to that of the external environment.

expresses the average glucose concentration within the cylindrical hydrogel cavity every second for 1 h at each of the external glucose concentrations. Physiological lag times upward of 15 min have been reported between glucose changes in the interstitial fluid (ISF) and in the blood.^{33–37} For the DNNC cylindrical hydrogel (diameter 1.5 mm, length 5 mm), an average lag time of 19.59 ± 0.13 min was observed and thus somewhat exceeds physiological lag. To reduce the lag time, the cylinder diameter may be reduced. For instance, when the model was applied to a DNNC cylindrical hydrogel with a reduced diameter (diameter 350 μm , length 5 mm), a lag time of less than 5 min was determined (Figure S2, Supporting Information).

Thermosensitivity. The extent and rate at which the DNNC cylindrical hydrogel deswells and reswells upon cyclically heating ($T > \text{VPTT}$) and cooling ($T < \text{VPTT}$) is important for its ability to function as a self-cleaning membrane for a subcutaneous glucose biosensor. First, the extent of deswelling is critical as this is the driving force behind physical removal of adhered cells on the membrane.^{9,14} When the

temperature was increased and maintained at ~ 40 °C for 1 h, the diameter of a vertically affixed DNNC cylinder decreased to $\sim 25\%$ of its initial swollen state diameter at RT (Figure 4).

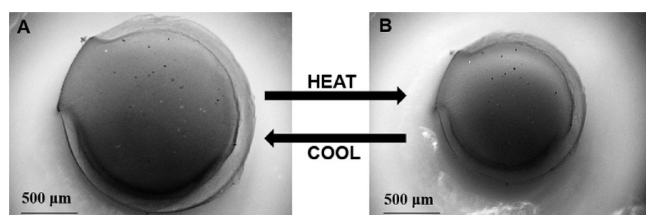


Figure 4. Bright field microscopy images of a vertically affixed DNNC cylinder in its swollen state at 25 °C ($T < VPTT$) [A] and deswollen state at 40 °C ($T > VPTT$) [B].

After returning to 25 °C for a period of 1 h, the diameter returned to within 5% of its initial measured swollen state diameter. Second, the membrane must be able to undergo cyclical deswelling/reswelling while being thermally cycled. This behavior was confirmed by subjecting a vertically affixed DNNC cylinder to cyclical heating (~ 1.06 °C/min) and cooling (~ 0.28 °C/min) over a 10 h period (Figure 5). Here, diameters achieved in the swollen and deswollen states remained very consistent.

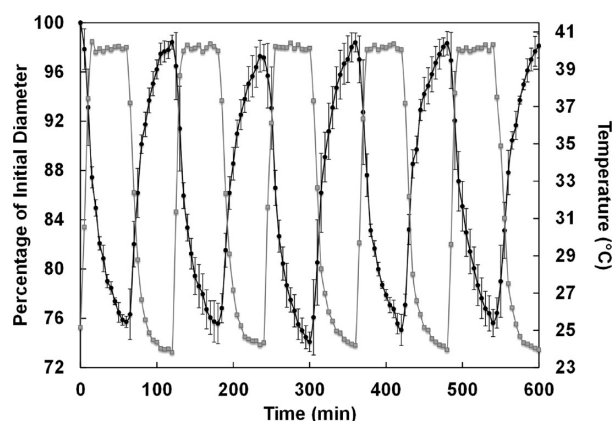


Figure 5. Diameter change during thermal cycling of a vertically affixed DNNC cylinder over a 10 h time period. Diameter change (black) and temperature change (gray).

Cytocompatibility. Cytocompatibility is essential to the utility of a self-cleaning membrane for a subcutaneously implanted glucose biosensor. The cytocompatibility of the DNNC hydrogel was determined via LDH activity assays (Figure 6). LDH is a soluble cytosolic enzyme that is released into the culture medium due to apoptosis or necrosis.³⁸ LDH levels released by 3T3 H2B-GFP mouse fibroblast cells 24 h postseeding were measured for the DNNC hydrogel and compared to that of noncytotoxic PEG-DA hydrogel and tissue culture plastic (i.e., PS). No statistical difference in normalized levels of exogenous LDH activity was observed. Thus, the DNNC hydrogel exhibits low cytotoxicity toward fibroblast cells similar to that of PEG-DA hydrogels.

“Self-Cleaning” in Vitro. The ability of the DNNC hydrogel to release adhered cells (i.e., self-clean) when induced to deswell with thermally heating was assessed in vitro against a nonthermoreponsive PEG-DA hydrogel control (Figure 7). To achieve adequate adhesion of fibroblasts, the DNNC and

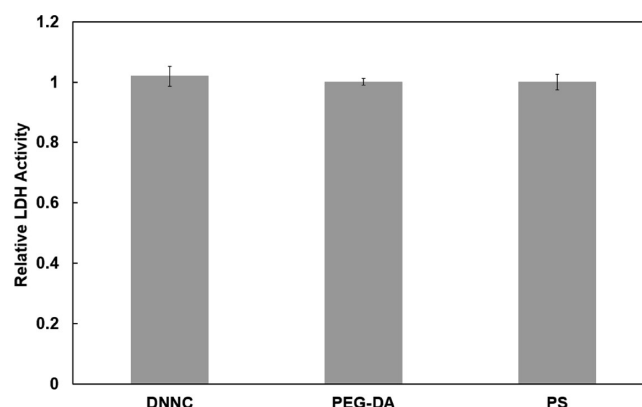


Figure 6. Relative LDH activity after 24 h for PEG-DA, DNNC, and polystyrene (PS) inoculated with 3T3 H2B-GFP mouse fibroblast cells.

PEG-DA hydrogel sheets were first exposed to DMEM (40% NCS) for 48 and 96 h, respectively. Such surface conditioning with protein is a common strategy to facilitate cellular adhesion.³⁹ This protocol also parallels the way in which an implanted surface first adsorbs proteins prior to the adhesion of cells.³ A longer conditioning period for PEG-DA hydrogels was determined to be required and can be attributed to the protein repulsive nature of PEG-DA.^{40,41} Initially, at ~ 35.4 °C ($T < VPTT$), both the DNNC and PEG-DA hydrogels were swollen and adhered fibroblasts exhibit a characteristic spread morphology. Heating to a temperature of ~ 39.5 °C was chosen as it is above the onset of the VPTT of the DNNC hydrogel and is below ~ 41 °C where protein denaturation may occur. Upon heating, the DNNC hydrogel underwent deswelling and fibroblasts display a round cell morphology indicative of end stages of detachment. In contrast, the PEG-DA hydrogel does not undergo appreciable deswelling and cells remained adhered. The percentage of attached cells on DNNC and PEG-DA hydrogels was assessed from four frames each taken while heating a single membrane from ~ 35 °C to ~ 39.5 °C ($T > VPTT$) over 10 min (Figure 7). Thus, while the PEG-DA hydrogel was more resistant to cellular adhesion, cell release was thermally triggered for the DNNC hydrogel.

CONCLUSIONS

A thermoresponsive DNNC hydrogel design was refined and evaluated for its ability to function as a self-cleaning membrane for a subcutaneously implanted glucose biosensor. The VPTT was adjusted to ~ 38 °C with NVP comonomer such that the membrane would be swollen at body temperature (35 °C, wrist subcutaneous tissue) to maximize glucose diffusion. Thus, when heated about the VPTT, the membrane would undergo reversible deswelling, which should detach adhered cells from its surface. Furthermore, the nondegradable nature of PNIPAAm hydrogels^{42,43} is expected to be advantageous to maintain membrane functionality and to sustain containment of sensing materials.

The measured glucose diffusion coefficient (D) for the DNNC membrane was within the physiological range at 35 °C but decreased substantially when the membrane was heated to ~ 40 °C and deswollen. Consequently, during this phase of self-cleaning, glucose measurements would not be effective. A cylindrical rod (~ 1.5 mm \times 5 mm, diameter \times length) was considered to be a suitable geometry for implantation. On the basis of a finite element model, glucose diffusion lag time for

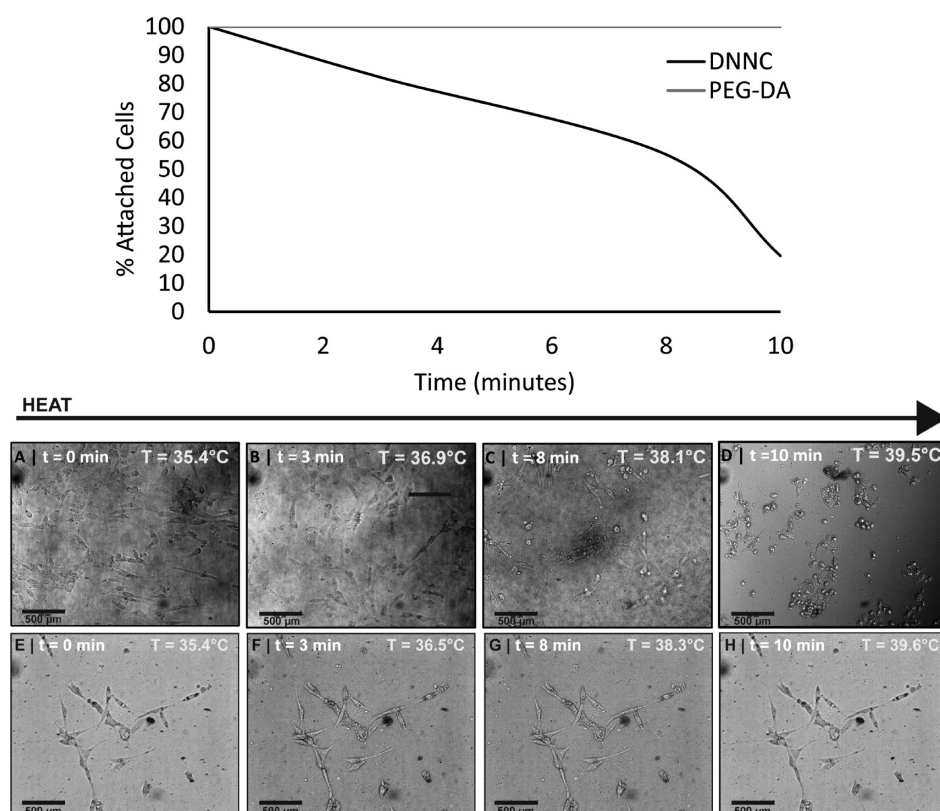


Figure 7. Bright field microscopy frames of DNNC [A–D] and PEG-DA [E–H] membranes seeded with 3T3 H2B-GFP mouse fibroblast cells incubated at $\sim 35^\circ\text{C}$ ($T < \text{VPTT}$) and then heated to $\sim 39.5^\circ\text{C}$ ($T > \text{VPTT}$). [A–D] demonstrate the detachment of cells due to deswelling of DNNC membrane. The graph depicts the percentage of attached cells to either DNNC or PEG-DA membranes as the temperature was increased from ~ 35 to $\sim 39.5^\circ\text{C}$ over a ~ 10 min period.

the DNNC hydrogel cylinders was estimated to be ~ 19 min. However, when a reduced diameter ($350\ \mu\text{m}$) was considered, the lag time was reduced to ~ 5 min.

Thermosensitivity, critical to self-cleaning efficacy, of the DNNC cylindrical hydrogel was assessed by measuring the change in diameter when in a deswollen ($T > \text{VPTT}$) versus swollen state ($T < \text{VPTT}$). Over a 10 h period of thermal cycling, the diameter of the deswollen cylindrical hydrogel returned to within 5% of the original swollen diameter.

In vitro, fibroblast cells exhibited minimal cytotoxicity and release from a planar DNNC hydrogel upon deswelling by heating above the VPTT while cells remained adhered to the nonthermoreponsive PEG-DA surface. In future studies, the release of other cell types as well as the adsorption of proteins will be conducted to thoroughly assess the self-cleaning behavior of the DNNC membrane.

■ ASSOCIATED CONTENT

● Supporting Information

Figure S1: DSC thermogram of the DNNC hydrogel; Figure S2: computational glucose diffusion model of a $350\ \mu\text{m}$ diameter cylindrical DNNC hydrogel. This material is available free of charge via the Internet at <http://pubs.acs.org>.

■ AUTHOR INFORMATION

Corresponding Author

*E-mail: mgrunlan@tamu.edu.

Notes

The authors declare no competing financial interest.

■ ACKNOWLEDGMENTS

Funding from the NIH/NIDDK (1R01DK095101-01A1) is gratefully acknowledged. We thank Prof. Michael McShane (Texas A&M University) for the use of his YSI 2700 Select Biochemistry Analyzer. Finally, we thank Prof. Arum Han (Texas A&M University) for the use of his Nikon Eclipse LV 100D noninverted bright field microscope.

■ REFERENCES

- (1) Shaw, J. E.; Sicree, R. A.; Zimmet, P. Z. *Diabetes Res. Clin. Pract.* **2010**, *87*, 4–14.
- (2) Rubin, R. R.; Peyrot, M. *Diabetes Metab. Res. Rev.* **1999**, *15*, 205–218.
- (3) Frost, M.; Meyerhoff, M. E. *Anal. Chem.* **2006**, *78*, 7370–7377.
- (4) Wisniewski, N.; Reichert, M. *Colloids Surf., B* **2000**, *18*, 197–219.
- (5) Quinn, C. A.; Connor, R. E.; Heller, A. *Biomaterials* **1997**, *18*, 1665–1670.
- (6) Marshall, A. J.; Ratner, B. D. *AIChE J.* **2005**, *51*, 1221–1232.
- (7) Bota, P. C. S.; Collie, A. M. B.; Puolakkainen, P.; Vernon, R. B.; Sage, E. H.; Ratner, B. D.; Stayton, P. S. *J. Biomed. Mater. Res. Part A* **2010**, *95*, 649–657.
- (8) Brauker, J. H.; Carr-Brendel, V. E.; Martinson, L. A.; Crudele, J.; Johnston, W. D.; Johnson, R. C. *J. Biomed. Mater. Res., Part A* **1995**, *29*, 1517–1524.
- (9) Okano, T.; Yamada, N.; Okuhara, M.; Sakai, H.; Sakurai, Y. *Biomaterials* **1995**, *16*, 297–303.
- (10) Kobayashi, J.; Okano, T. *Sci. Technol. Adv. Mater.* **2010**, *11*, 014111.
- (11) Yang, J.; Yamato, M.; Nishida, K.; Ohki, T.; Kanzaki, M.; Sekine, H.; Shimizu, T.; Okano, T. *J. Controlled Release* **2006**, *116*, 193–203.
- (12) Tang, Z.; Akiyama, Y.; Okano, T. *Polymers* **2012**, *4*, 1478–1498.

- (13) Gant, R. M.; Hou, Y.; Grunlan, M. A.; Cote, G. L. *J. Biomed. Mater. Res., Part A* **2009**, *90*, 695–701.
- (14) Hou, Y.; Matthews, A. R.; Smitherman, A. M.; Bulick, A. S.; Hahn, M. S.; Hou, H.; Han, A.; Grunlan, M. A. *Biomaterials* **2008**, *29*, 3175–3184.
- (15) Haraguchi, K.; Li, H.-J. *Macromolecules* **2006**, *39*, 1898–1905.
- (16) Zhang, X.-Z.; Xu, X.-D.; Cheng, S.-X.; Zhuo, R.-X. *Soft Matter* **2008**, *4*, 385–391.
- (17) Fei, R.; George, J. T.; Park, J.; Grunlan, M. A. *Soft Matter* **2011**, *8*, 481–487.
- (18) Montgomery, L. D.; Williams, B. A. *Ann. Biomed. Eng.* **1976**, *4*, 209–219.
- (19) Werner, J.; Buse, M. *J. Appl. Physiol.* **1988**, *65*, 1110–1118.
- (20) Erbil, C.; Aras, S.; Uyanik, N. *J. Polym. Sci., Part A: Polym. Chem.* **1999**, *37*, 1847–1855.
- (21) Feil, H.; Bae, Y. H.; Feijen, J.; Kim, S. W. *Macromolecules* **1993**, *26*, 2496–2500.
- (22) Gant, R. M.; Abraham, A. A.; Hou, Y.; Cummins, B. M.; Grunlan, M. A.; Cote, G. L. *Acta Biomater.* **2010**, 2903–2910.
- (23) Wu, C.; Zhou, S. *Macromolecules* **1997**, *30*, 574–576.
- (24) Bao, L.-R.; Cheng, X.; Huang, X. D.; Guo, L. J.; Pang, S. W.; Yee, A. F. *J. Vac. Sci. Technol., B* **2002**, *20*, 2881–2886.
- (25) Hannoun, B. J.; Stephanopoulos, G. *Biotechnol. Bioeng.* **1986**, *28*, 829–835.
- (26) Teixeira, J. A.; Mota, M.; Venâncio, A. *Chem. Eng. J.* **1994**, *56*, B9–B14.
- (27) Venancio, A.; Teixeira, J. A. *Biotechnol. Tech.* **1997**, *11*, 183–185.
- (28) Zhang, W.; Furusaki, S. *Biochem. Eng. J.* **2001**, *9*, 73–82.
- (29) Khalil, E.; Kretsos, K.; Kasting, G. B. *Pharm. Res.* **2006**, *23*, 1227–1234.
- (30) Russell, R. J.; Axel, A. C.; Shields, K. L.; Pishko, M. V. *Polymer* **2001**, *42*, 4893–4901.
- (31) Quinn, C. P.; Pishko, M. V.; Schmidtke, D. W.; Ishikawa, M.; Wagner, J. G.; Raskin, P.; Hubbell, J. A.; Heller, A. *Am. J. Physiol.* **1995**, *269*, E155–E161.
- (32) Tuchin, V. V. *Handbook of Optical Sensing of Glucose in Biological Fluids and Tissues*; CRC Press: Boca Raton, 2009; p xxxii, 709 p.
- (33) Aussedat, B.; Dupire-Angel, M.; Gifford, R.; Klein, J. C.; Wilson, G. S.; Reach, G. *Am. J. Physiol.* **2000**, *278*, E716–E728.
- (34) Baker, D. A.; Gough, D. A. *Anal. Chem.* **1996**, *68*, 1292–1297.
- (35) Heise, T.; Koschinsky, T.; Heinemann, L.; Ludwig, V. *Diabetes Technol. Ther.* **2003**, *5*, 563–571.
- (36) Rebrin, K.; Steil, G. M. *Diabetes Technol. Ther.* **2000**, *2*, 461–472.
- (37) Rebrin, K.; Steil, G. M.; van Antwerp, W. P.; Mastrototaro, J. J. *Am. J. Physiol.* **1999**, *277*, E561–E571.
- (38) Renner, K.; Amberger, A.; Konwalinka, G.; Kofler, R.; Gnaiger, E. *Biochim. Biophys. Acta, Mol. Cell Res.* **2003**, *1642*, 115–123.
- (39) Grinnell, F.; Feld, M. K. *J. Biol. Chem.* **1982**, *257*, 4888–4893.
- (40) Gombotz, W. R.; Guanghui, W.; Hoffman, A. S. *J. Biomed. Mater. Res.* **1991**, *25*, 1547–1562.
- (41) Jeon, S. I.; Andrade, J. D. *J. Colloid Interface Sci.* **1991**, *142*, 159–166.
- (42) Patenaude, M.; Hoare, T. *Biomacromolecules* **2012**, *13*, 369–378.
- (43) Klouda, L.; Mikos, A. G. *Eur. J. Pharm. Biopharm.* **2008**, *68*, 34–45.